

Supplementary Materials for “Tunable Magnetic and Electronic Properties of CrS₂/VS₂ Lateral Superlattices”

Huimin Gao,¹ Yimei Fang,² Yinghui Zhou,^{1,*} Feng Zheng,² Tie-Yu Lü,¹ Xinrui Cao,^{1,3} Zi-zhong Zhu,^{1,3} and Shunqing Wu^{1,*}

¹*Department of Physics, OSED, Key Laboratory of Low Dimensional Condensed Matter Physics (Department of Education of Fujian Province), Xiamen University, Xiamen 361005, China*

²*School of Science, Jimei University, Xiamen 361021, China*

³*Fujian Provincial Key Laboratory of Theoretical and Computational Chemistry, Xiamen University, Xiamen 361005, China*

Content

Figure S1. The energy differences between the ferromagnetic and antiferromagnetic states of monolayers (a) 1T-CrS₂ and (b) 2H-VS₂ for different effective U values.

Figure S2. Band structures and density of states of monolayer CrS₂ and VS₂.

Figure S3. The formation energy of the lateral superlattice CrS₂(*m*)/VS₂(*n*) (*m*+*n*=14) as a function of the width (*m*) of the CrS₂ sublattice.

Figure S4. The energy profiles of various magnetic configurations evolve as a function of the number of units for *m*+*n*=13.

Figure S5. Top view of monolayers (a) 1T-CrS₂ and (b) 2H-VS₂. The orange and green arrows correspond to lattice constants *a* and *b*. The red arcs represent the Cr-S-Cr (V-S-V) angles θ_1 and θ_2 , respectively.

Figure S6. Schematic diagrams illustrating three magnetic orders used for the calculation of exchange parameters: (a) FM, (b) FM&AFM, (c) AFM1 and (d) AFM2.

Figure S7. Projected density of states of the central unit cells of CrS₂ and VS₂ in the CrS₂(7)/VS₂(7) superlattice.

Figure S8. The charge transfer at the interface from the CrS₂ ribbon to the VS₂ ribbon as a function of the number of units for *m*=*n*.

Figure S9. Projected density of states of the central unit cells of CrS₂ and VS₂ in the CrS₂(1)/VS₂(13) and CrS₂(13)/VS₂(1) superlattices.

* Email: wsgq@xmu.edu.cn (S.Q.W.); yhzhou@xmu.edu.cn (Y.H.Z.)

Table S1. Structural parameters of the FM and sAFM states for monolayers 1T-CrS₂ and 2H-VS₂.

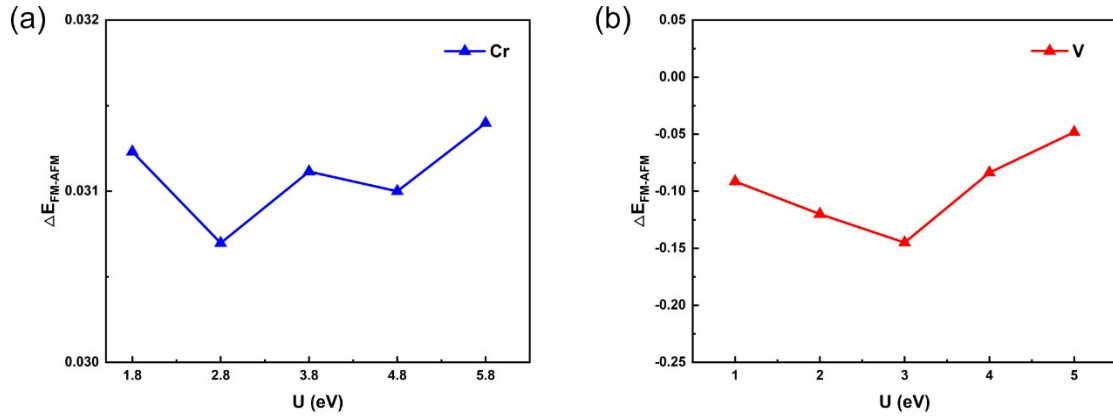


Figure S1. The energy differences between the ferromagnetic and antiferromagnetic states of monolayers (a) 1T-CrS₂ and (b) 2H-VS₂ for different effective U values.

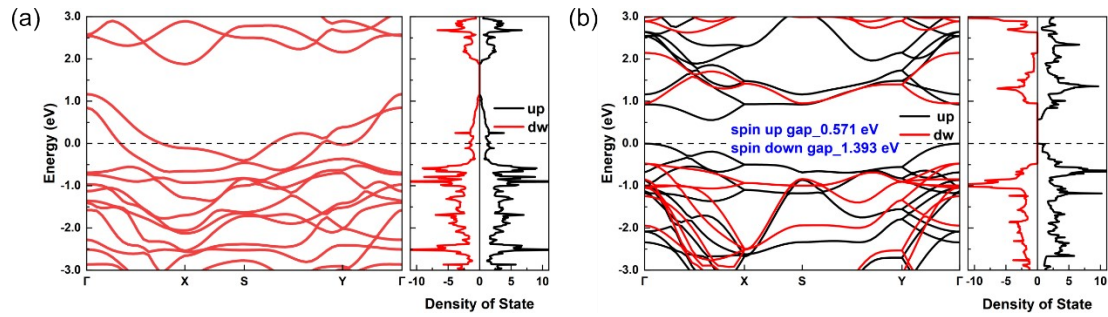


Figure S2. Band structures and density of states of monolayer (a) CrS₂ and (b) VS₂.

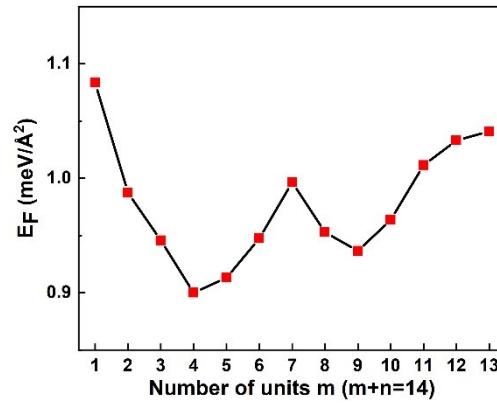


Figure S3. The formation energy of the lateral superlattice $\text{CrS}_2(m)/\text{VS}_2(n)$ ($m+n=14$) as a function of the width (m) of the CrS_2 sublattice.

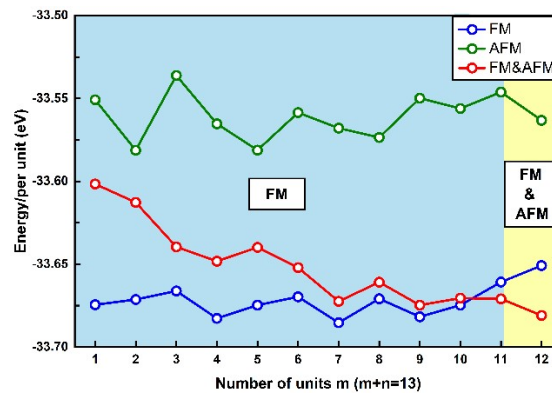


Figure S4. The energy profiles of various magnetic configurations evolve as a function of the number of units for $m+n=13$.

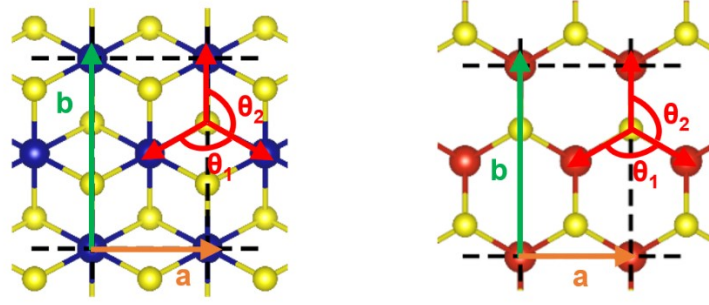


Figure S5. Top view of monolayers (a) 1T-CrS₂ and (b) 2H-VS₂. The orange and green arrows correspond to lattice constants a and b . The red arcs represent the Cr-S-Cr (V-S-V) angles θ_1 and θ_2 , respectively.

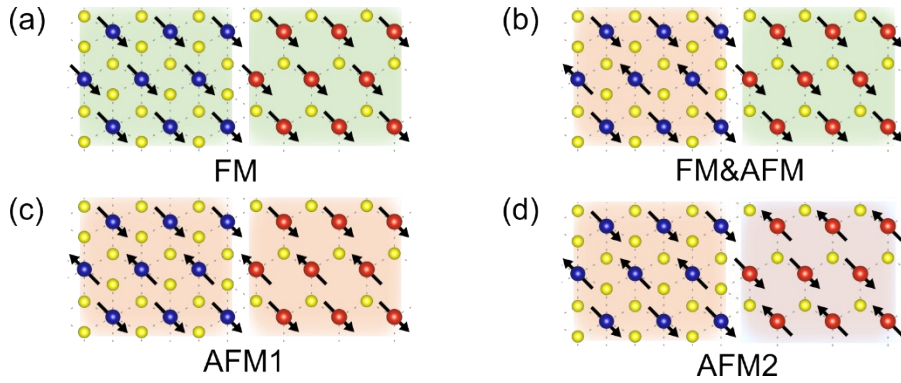


Figure S6. Schematic diagrams illustrating three magnetic orders used for the calculation of exchange parameters: (a) FM, (b) FM&AFM, (c) AFM1 and (d) AFM2.

Spin-exchange coupling parameters (see Fig. 4(a)) were extracted by calculating the total energy differences of eight magnetic configurations (see Fig. S4(a)-(d)) based on the Heisenberg model. The energy contributed by magnetic interaction in these magnetic orders in a unit cell is expressed as

$$E_1 = -2 \times (m-1) \times S_{Cr}^2 \times 3J_1 - 2 \times (n-1) \times S_V^2 \times 3J_2 - 2 \times S_{Cr}S_V \times 3J_3 + H_0$$

$$E_2 = 2 \times (m-1) \times S_{Cr}^2 \times J_1 - 2 \times (n-1) \times S_V^2 \times 3J_2 + 2 \times S_{Cr}S_V \times 3J_3 + H_0$$

$$E_3 = 2 \times (m-1) \times S_{Cr}^2 \times J_1 + 2 \times (n-1) \times S_V^2 \times J_2 + 2 \times S_{Cr}S_V \times 3J_3 + H_0$$

$$E_4 = 2 \times (m-1) \times S_{Cr}^2 \times J_1 + 2 \times (n-1) \times S_V^2 \times J_2 - 2 \times S_{Cr}S_V \times 3J_3 + H_0 \text{(S1)}$$

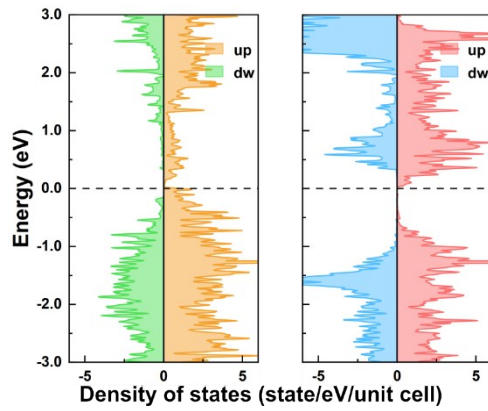


Figure S7. Projected density of states of the central unit cells of CrS_2 and VS_2 in the $\text{CrS}_2(7)/\text{VS}_2(7)$ superlattice.

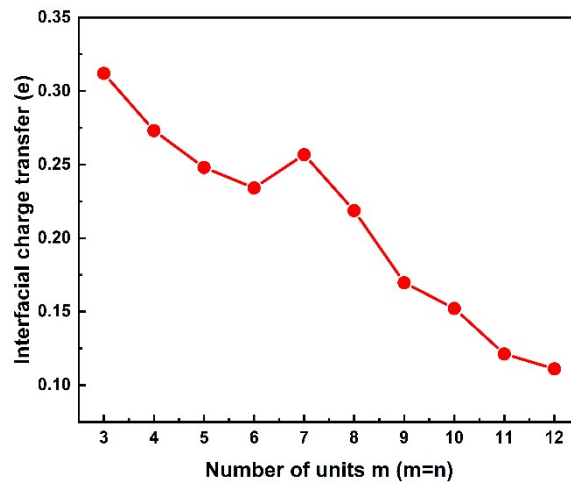


Figure S8. The charge transfer at the interface from the CrS_2 ribbon to the VS_2 ribbon as a function of the number of units for $m=n$.

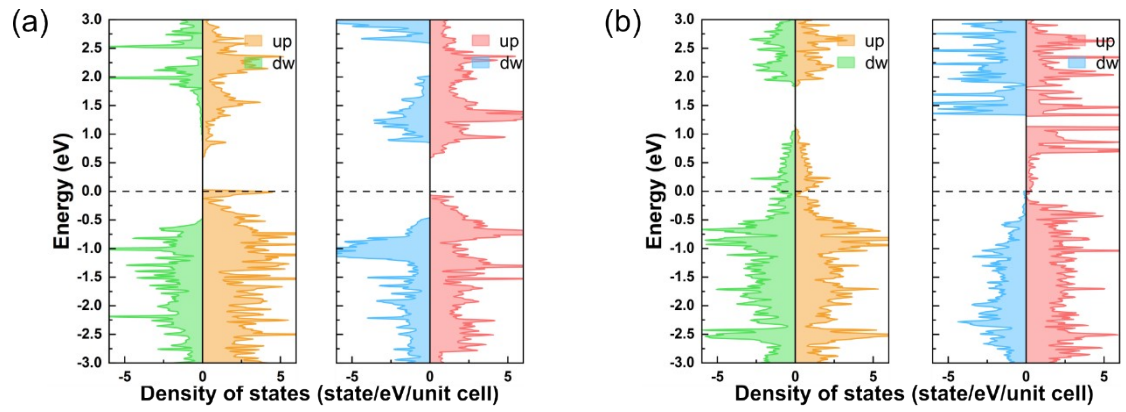


Figure S9. Projected density of states of the central unit cells of CrS₂ and VS₂ in the (a) CrS₂(1)/VS₂(13) and (b) CrS₂(13)/VS₂(1) superlattices.

Table S1. Structural parameters of the FM and sAFM states for monolayers 1T-CrS₂ and 2H-VS₂.

	a (Å)	b (Å)	θ_1 (°)	θ_2 (°)
CrS ₂ -sAFM	3.34	5.51	88.58	84.85
CrS ₂ -FM	3.33	5.76	88.61	88.21
VS ₂ -sAFM	3.22	5.64	86.42	86.20
VS ₂ -FM	3.22	5.57	87.66	87.62